### DYNAMIC DE-EXCITATION PERFORMANCE OF BRUSHLESS SYNCHRONOUS MACHINES USING ADVANCED CONTROL STRATEGY

SEIF EDDINE CHOUABA<sup>1</sup>, ABDALLAH BARAKAT<sup>2</sup>

Keywords: Synchronous generator; Brushless excitation; Voltage regulation; H∞ control; Fuzzy logic controller.

Synchronous generators (SG) are key electromechanical converters widely used in power plants, where precise excitation control is crucial for maintaining voltage regulation and stability. The main limitation of the conventional brushless excitation (CBE) system is its inability to supply negative voltages to the field winding, which limits fast de-excitation during sudden load rejection and causes terminal-voltage overshoots. To address this issue, this paper proposes an advanced fuzzy brushless excitation (FABE) system integrating fuzzy logic control (FLC) with  $H^{\infty}$  control to enhance the transient and steady-state performance of synchronous generators. The  $H^{\infty}$  controller ensures robustness against disturbances, parameter uncertainties, and nonlinearities, while the FLC improves adaptability and dynamic response. The proposed hybrid approach enables faster de-excitation, reduced voltage peaks, and improved damping of oscillations. Simulation results demonstrate that the FABE system clearly outperforms the conventional excitation method in terms of voltage stability, dynamic response, and overall control performance under various operating conditions.

#### 1. INTRODUCTION

Brushless synchronous machines play a crucial role in various industrial applications, including power generation, automotive, and marine industries, due to their efficiency and reliability [1]. However, ensuring optimal performance, particularly in dynamic de-excitation scenarios, remains a challenge. Dynamic de-excitation is the process of rapidly reducing the excitation voltage of the generator's field winding to prevent voltage overshoots and maintain system stability during sudden changes in load or faults [2-8]. Among the various de-excitation systems developed for brushless synchronous machines, some incorporate a discharge resistor positioned between the field winding and the rotating diode bridge. These systems play a critical role in ensuring safe operation and efficient protection of these machines. Some research studies and industrial efforts have concentrated on optimizing the brushless excitation system to generate a negative excitation voltage. In reference [2], the negative excitation capability is achieved through selfactuated de-excitation impedance on the shaft. It is worth noting that this technique primarily focuses on rapidly demagnetizing the system to cease excitation after fault detection (such as a short circuit). However, the deexcitation system proposed in these studies lacks the ability to be controlled using a closed-loop control strategy for dynamic voltage regulation. The authors in [3] have introduced a method to enhance transient de-excitation in brushless synchronous machines. This method involves the integration and demonstration of a system that combines a high-speed brushless de-excitation system with a static field breaker to ameliorate the transient response of synchronous machines. In reference [4], it was proposed to employ the fast de-excitation system not only for the main generator but also for the exciter machine, resulting in a further reduction in de-excitation time. Recently, in 2023, the authors proposed a de-excitation system for brushless excitation based on a synchronous generator. This system employs a discharge resistor in series with a freewheeling diode of a buck chopper. Furthermore, the authors outline a methodology for determining the suitable value of the discharge resistance [7].

The control techniques used for the de-excitation system of brushless synchronous machines vary depending on the specific design and operational requirements. Some common classical control approaches include linear PID control and hysteresis comparator methods [5,6]. However, classical controllers often face limitations when dealing with nonlinearities and parameter variations inherent to electrical machines. Fuzzy logic controllers (FLC) are well recognized for their ability to incorporate human expertise, intuition, and heuristics into the control process, rather than relying solely on precise mathematical models. This feature makes them highly effective in power system applications [9-12], particularly when system models are uncertain or poorly defined [13]. Their ability to manage nonlinear dynamics, input fluctuations, and environmental variations renders them suitable for complex and variable operating conditions. Nevertheless, their implementation may impose significant computational burdens, especially when many fuzzy inputs increase the rule base size [14]. Despite these drawbacks, fuzzy logic remains more robust and adaptive than conventional PID controllers. In this context, the present paper introduces an innovative de-excitation control strategy for brushless synchronous generators that combines Fuzzy logic control (FLC) with H∞ control, ensuring both adaptability and robust stability under various operational conditions. The H∞ regulator, as demonstrated in recent studies on robust power system stabilization [15], provides strong resilience against disturbances and model uncertainties. The proposed hybrid control approach is validated through simulation tests focusing on key performance metrics such as voltage overshoot, response time, and system stability. The paper is organized as follows: Section 2 introduces the principles of dynamic excitation and de-excitation in brushless synchronous generators. Section 3 describes the proposed control strategy combining FLC and H∞ controllers. Section 4 presents the validation and performance analysis of the proposed excitation system through various simulations conducted on an 11.2 kVA synchronous generator. Finally, Section 5 concludes the paper.

# 2. PRINCIPLE OF DYNAMIC EXCITATION AND DE-EXCITATION IN BRUSHLESS SYNCHRONOUS MACHINES

In this section, we provide an overview of the dynamic excitation/de-excitation system employed in brushless synchronous machines. For a more comprehensive understanding, readers are encouraged to consult the

<sup>&</sup>lt;sup>1</sup> DAC-HR Laboratory, University of Setif 1, Sétif, 19000, Algeria. E-mail: seif.chouaba@univ-setif.dz

<sup>&</sup>lt;sup>2</sup> IREENA, Université de Nantes, Nantes, 44000, France. E-mail: abdallah.barakat@univ-nantes.fr

references [5,6]. Figure 1 illustrates the block diagram outlining the components involved in the dynamic brushless excitation/de-excitation system. The system achieves complete excitation control through:

- Positive excitation control: This involves regulating the excitation current of the exciter machine.
- Negative excitation (de-excitation): This is achieved by controlling the opening and closing of the rotating IGBT. Opening the IGBT introduces the rotating discharge resistor (Rd), applying a negative excitation voltage across the generator's field winding.

An IGBT device is chosen for its widespread use in power applications. The proposed de-excitation system offers the advantage of transmitting the activation and deactivation signals of the IGBT through a brushless control system. This system comprises a low-power rotating diode paired with a low-power control machine (CM), which is an inverse synchronous machine. The voltage regulator manages the excitation current of the control machine using a low-power

DC chopper. This solution is resistant to electromagnetic interference and eliminates the need for brushes. Material selection for the machine must consider the requirement for swift control signal transmission. The excitation/de-excitation system enables robust control of the main generator field winding with both positive and negative voltages, without requiring brushes. This Fuzzy Advanced Brushless Excitation structure can be utilized in various scenarios:

- Routine shutdowns: to reduce the duration of the synchronous generator (SG) excitation current.
- Following fault detection: to swiftly reduce the SG excitation current.
- Enhancing dynamic performance: during abrupt load rejections, the introduction of the discharge resistor introduces a negative excitation voltage, enabling rapid reduction of the field current and minimizing generator voltage overshoot.

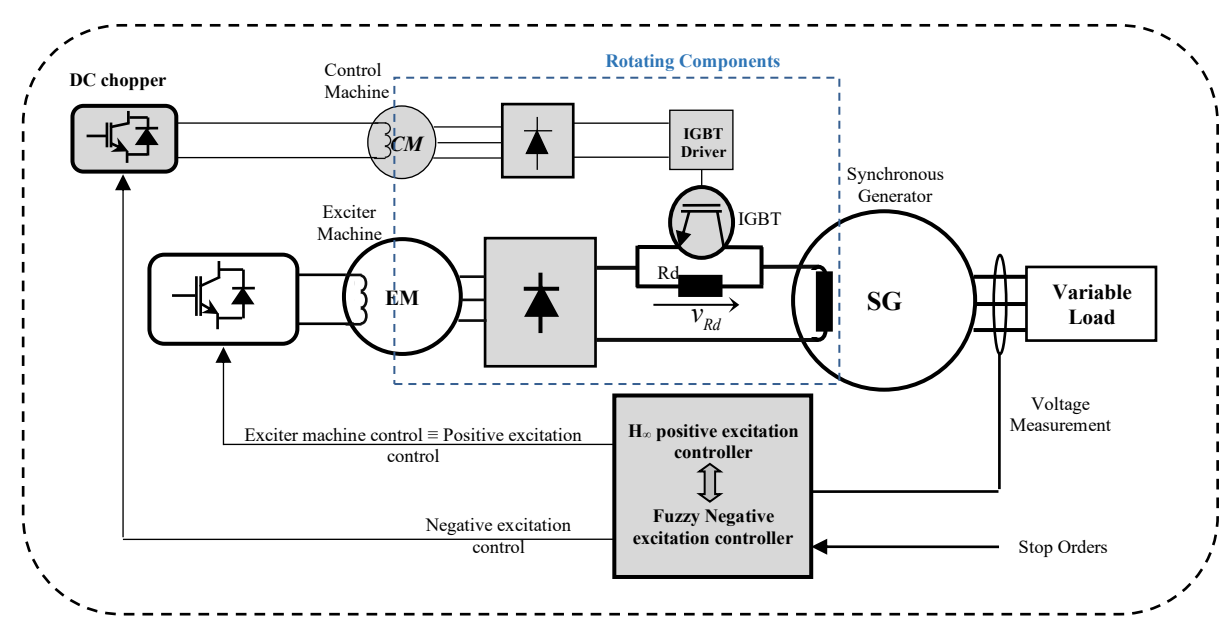


Fig. 1 – Overview of the components of the dynamic brushless excitation/de-excitation system.

## 3. DE-EXCITATION/ EXCITATION SYSTEM CONTROLLERS DESIGN

The control mechanism for the opening and closing of the IGBT relies on an FLC. Additionally, the  $H\infty$  voltage regulator excitation design treats the IGBT status as a perturbation to be rejected. This integrated approach ensures system stability in closed-loop operation.

### 3.1 DYNAMIC DE-EXCITATION FUZZY LOGIC CONTROL STRATEGY

A fast de-excitation system increases the dynamic behavior of the global system and reduces the voltage overshoots during load rejections. In this work, we use fuzzy logic control for the high voltage overshoot based on the rotating IGBT with the discharge resistor. The IGBT opening and closing control is based on a fuzzy logic controller. A fuzzy logic regulator is selected for its sensitivity and adaptability based on the specific application requirements. Fig. 2 illustrates the block diagram of the fuzzy logic de-

excitation control system. The inputs to the regulator include the error signal e(t), which represents the variance between the reference value  $U_{2ref}$  and the measured generator voltage  $U_{mes}$ , delta error de(t). The output of this controller is  $U_{IGBT}$ , which controls the opening and closing of the IGBT.

$$\begin{cases} e(t) = U_{2ref} - U_{mes} \\ de(t) = e(t) - e(t-1) \end{cases}$$
 (1)

G1 and G2 represent scaling factors where the gains of the error input and its derivative are adjusted. These factors are varied until a suitable tuning phenomenon is found. They also allow changing the sensitivity of the fuzzy controller without altering its structure. The evaluation of gains comes from experience, and these values are part of the evaluation procedure through simulation. Indeed, they have a significant effect on the static and dynamic performance of the control.

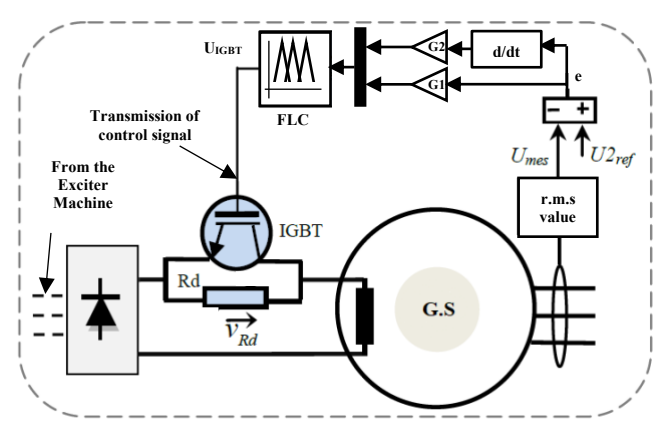
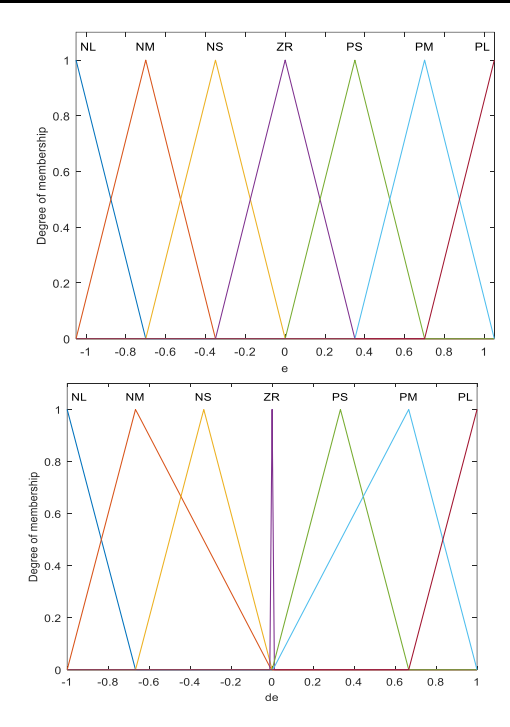


Fig. 2 - Block diagram of the FLC system used for de-excitation.

In this study, the Mamdani-type is utilized to convert the inputs into appropriate fuzzy linguistic sets. These fuzzy sets are then processed in the inference system, where appropriate fuzzy output is determined based on fuzzy rules, and the fuzzy output is converted into a crisp value in the defuzzification using the center of gravity approach [14]. The membership functions for the inputs and the output variables are triangular membership functions named: NL, NM, NS, ZR, PS, PM, and PL. In total, this design incorporates 49 fuzzy rules, as presented in Table 1 and depicted in the graphs in Fig. 3.

Table 1
Rules table for fuzzy inference system

e de	NL	NM	NS	ZR	PS	PM	PL
NL	NL	NL	NL	NS	PS	PS	PS
NM	NL	NL	NL	NP	PS	PS	PS
NS	NL	NL	NM	NS	PS	PS	PM
ZR	NL	NM	NS	ZR	PS	PM	PL
PS	NM	NS	NS	PS	PM	PL	PL
PM	NS	NP	NP	PS	PM	PL	PL
PL	NS	NP	NP	PS	PL	PL	PL



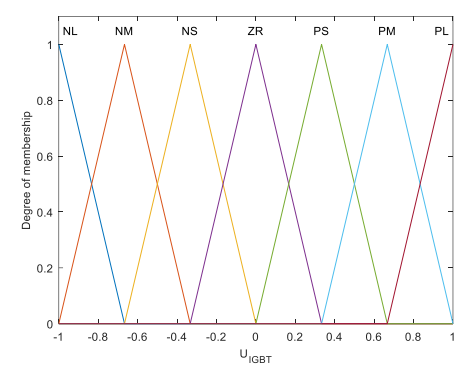


Fig. 3 – The membership functions for the inputs and output of the FLC de-excitation system.

The conditions for seven sets of rules are used to minimize the error and enhance their dynamic response. In prior work [5], the control of the opening and closing of the IGBT was managed using a PI-controller and a hysteresis comparator. However, their slow tuning process presented difficulties in effectively controlling both the timing and magnitude of the transient synchronous generator voltage. To address this issue, a fuzzy controller has been introduced to minimize the de-excitation system error within the control loop governing the opening and closing of the IGBT associated with the rotating discharge resistor ( $R_d$ ).

#### 3.2 DYNAMIC EXCITATION CONTROL STRATEGY

In this paper, we implemented an  $H\infty$  voltage regulator in both the CBE and FABE systems. The  $H\infty$  regulator is constructed based on the mathematical model describing the behavior of the entire system, including the exciter machine, rotating diodes, main generator, and any unknown loads, which is validated experimentally in [16].

### 3.2.1 MATHEMATICAL EQUATIONS OF THE SYSTEM

The mathematical model of the system is described by the following equations:

$$v_{exc} = R_e i_{exc} + L_e \frac{di_{exc}}{dt} - (k_2 k_3) M_{se} \frac{di_f}{dt}$$
. (2.1)

$$i_{d1} = i_{dp} + C_1 \omega_{ep} v_{qp} - C_1 \frac{dv_{dp}}{dt}$$
 (2.2)

$$i_{q1} = i_{qp} - C_1 \omega_{ep} v_{dp} - C_1 \frac{dv_{qp}}{dt}$$
 (2.3)

$$0 = -v_{dp} - R_s i_{dp} + L_q \omega_{ep} i_{qp} - M_{sQ} \omega_{ep} i_Q - L_d \frac{di_{dp}}{dt}$$

$$+M_{sf}\frac{di_f}{dt}+M_{sD}\frac{di_D}{dt}$$

(2.4)

$$0 = -v_{qp} - R_s i_{qp} - L_d \omega_{ep} i_{dp} + M_{sf} \omega_{ep} i_f + M_{sD} \omega_{ep} i_D$$

$$-L_q \frac{di_{qp}}{dt} + M_{sQ} \frac{di_Q}{dt}$$
(2.5)

$$0 = -k_1 M_{se} \omega_{ee} i_{exc} + a i_f + L_f \frac{d i_f}{d t} - M_{sf} \frac{d i_{dp}}{d t} + M_{fD} \frac{d i_D}{d t}$$
 (2.6)

$$0 = R_D i_D + L_D \frac{di_D}{dt} + M_{fD} \frac{di_f}{dt} - M_{sD} \frac{di_{dp}}{dt}$$
 (2.7)

$$0 = R_{Q}i_{Q} + L_{Q}\frac{di_{Q}}{dt} - M_{sQ}\frac{di_{qp}}{dt}$$
(2.8)

This model has several parameters:

- $R_e$  and  $L_e$  denote respectively the resistance and the inductance of the EM field winding,
- $R_s$ ,  $L_f$ , and  $R_f$  are respectively the SG stator resistance, the field winding inductance, and the field winding resistance.
- $L_d$  and  $L_q$  are respectively the direct and the transverse stator inductance,
- $R_D$ ,  $R_Q$ ,  $L_D$ , and  $L_Q$  are respectively the direct and transverse dampers' resistances and the direct and transverse dampers' inductances.
- M<sub>sf</sub> and M<sub>fD</sub> are respectively the mutual inductance between the direct stator winding and field winding, and the mutual inductance between the field winding and the direct damper winding.
- M<sub>sQ</sub> and M<sub>sD</sub> are respectively the mutual inductance between the direct stator winding and the transverse damper winding, and the mutual inductance between the stator and the direct damper.
- ω<sub>ee</sub> and ω<sub>ep</sub> are the electrical angular speeds of the SG and the EM, respectively.
- C1 represents a virtual three-phase capacitor added at the SG terminal to model the load current as a perturbation to be rejected by the voltage regulator.

Additionally, in the provided equation,  $k_1$ ,  $k_4$ , and  $k_3$  are constants determined by the rectifier's electromagnetic parameters (such as leakage inductances and main inductance) and its operational mode.  $k_2$  serves as a correction factor, elaborated further in [16]. id1 and id2 denote the load currents in the dq frame, while  $v_{\rm exc}$  and  $i_{\rm exc}$  represent the excitation voltage and excitation current of the electromagnetic system, respectively. The variables  $v_{\rm dq}$ ,  $v_{\rm dq}$ ,  $i_{\rm dq}$ , and  $i_{\rm dq}$  correspond to the generator voltages and currents in the dq frame.  $i_{\rm D}$  and  $i_{\rm Q}$  signify the direct and quadrature dampers currents, respectively, and  $i_{\rm f}$  denotes the current of the synchronous generator's main field winding.

In the FABE system, the presence of the IGBT and the discharge resistor introduces additional factors affecting the generator voltage and system stability. To maintain stability during the IGBT opening and closing, we model the IGBT and linear discharge resistor as a variable voltage  $V_{Rd}$  connected in series with the main field winding of the synchronous generator (as illustrated in Fig. 2). Furthermore,  $V_{Rd}$  is treated as an exogenous input. In this scenario, the opening and closing of the IGBT, governed by the negative excitation controller, are perceived as disturbances to be counteracted by the positive excitation controller. This approach ensures stable operation in the presence of both positive and negative controllers.

$$V_{R_d} = \begin{cases} 0 & (when the IGBT is close) \\ -R_d \cdot If & (when the IGBT is open) \end{cases}$$
 (3)

#### 3.2.2 H∞ VOLTAGE REGULATOR DESIGN

From the mathematical model of the global system,  $H\infty$  feedback control system is used to synthesize a voltage regulator. The  $H\infty$  voltage regulator is formulated through the utilization of weighting filters W1(s) and W2(s), which are designed to shape both the disturbances and the system outputs [17]. Figure 4 illustrates the representation of the complete

system incorporating the H\infty voltage corrector K(s) and the weighting filters. This configuration yields the augmented plant P(s), which is used to design the H $\infty$  controller. The plant P(s) comprises two inputs: the exogenous input vector w, encompassing disturbances to be rejected, and the voltage reference (id1, iq1, V<sub>Rd</sub>, and U<sub>1ref</sub>). Additionally, z denotes the signals to be controlled, including the weighted error and the weighted control signal u. W1(s) typically functions as a lowpass filter of the first order. In contrast, the selection of W2(s) as a scalar weighting (constant) enables complete manipulation of the dynamics of the control signal [17]. The objective of H∞ control is to determine a controller K(s) that ensures system stability and minimizes the H $\infty$  norm of  $T_{zw}(s)$ , the closed-loop transfer function from the input w to the output z.  $T_{zw}(s)$  remains stable, and  $||T_{zw}|| \infty$  is minimized to constrain the maximum of all sensitivities below a certain value. How controllers are directly derived from the augmented plant P(s) using the hinfsyn function of the Robust Control Toolbox in MATLAB [18].

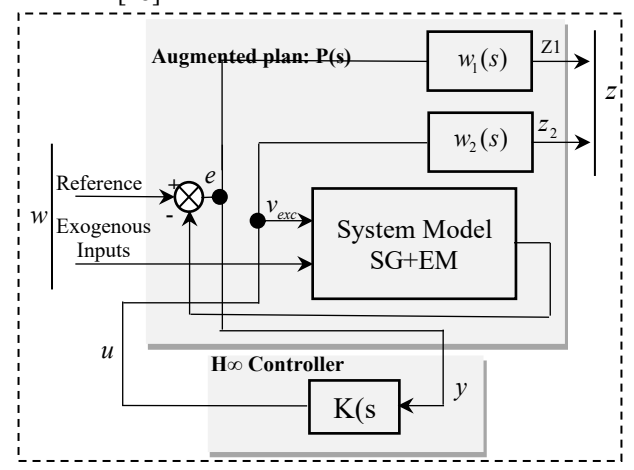


Fig. 4 – Standard representation for structured  $H\infty$  synthesis with augmented plant.

### 4. VALIDATION OF THE PROPOSED EXCITATION/DEEXCITATION SYSTEM

In this study, we utilize a realistic model of a brushless excitation system coupled with a synchronous generator, which has been developed, identified, and validated in [16]. The parameters of this system are provided in Appendix I. This model exhibits sufficient accuracy for both steady-state and dynamic conditions, including transient states. The experiments detailed in this paper were conducted using an 11.2 kVA synchronous generator, with a linear discharge resistor employed. Dynamic de-excitation tests, particularly during sudden load shedding, are performed on both the Conventional Brushless Excitation CBE system and the proposed FABE system. In this control model, the discrepancy between the measured generator voltage U<sub>mes</sub> and its reference value U<sub>2ref</sub> is fed into the FLC block. The reference voltage U<sub>2ref</sub> is typically set at 105% of the generator's nominal voltage. Under steady-state conditions, the measured generator voltage is regulated by the positive controller at U<sub>1ref</sub>, usually set to 100%. Drawing from various excitation system control strategies, we investigate different approaches for transmitting commands to open and close the rotating IGBT. These methods may include wireless communication, a brush ring system, capacitive coupling, and others. However, in this study, we directly apply external signal voltage control, comprising opening and closing commands, to the rotating IGBT. During this test, we analyze the stability and performance of voltage regulation in the FABE system under sudden load application and rejection. Table 2 outlines the loads used during impact and shedding tests, where P represents the load active power, S denotes the load apparent power, Q indicates the load reactive power, and PF represents the load power factor. To assess the effectiveness of the proposed FABE system in dynamic deexcitation, four tests are conducted and detailed in Table 2.

TABLE 2
Used load during the impact/shedding tests.

			0	
Tests	P (kW)	S (kVA)	Q (kVAR)	PF
$100_{0.8}$	8.96	11.2	6.72	0.8
$100_{0.3}$	6.72	11.2	8.96	0.3
$100_{0.6}$	3.36	11.2	10.6	0.6
$150_{0.8}$	13.4	16.8	10	0.8

To facilitate clear comparison of system responses, we'll utilize the root mean square (r.m.s.) value of the terminal voltage (per unit). Figures 5, 6, 7, and 8 depict the comparative behaviors of two systems: CBE and FABE during shedding scenarios. In these illustrations, green curves represent CBE response, while blue curves represent FABE response, incorporating fuzzy logic feedback control. The performance of FABE systems surpasses that of CBE systems in terms of voltage overshoot and response time. This enhancement primarily stems from the FABE structure's ability to provide the generator's main field winding with negative excitation voltage, facilitating rapid de-excitation of the generator field winding. Additionally, system stability is upheld through the H∞ design, which accounts for IGBT operation as a perturbation to be rejected. The CBE configuration lacks the capability to provide negative excitation voltage to the generator field winding, thus failing to mitigate voltage overshoot during shedding tests. Conversely, the FABE system can counteract voltage overshoot by directly introducing negative excitation voltage to the generator field winding through the opening of the rotating IGBT as needed. Figures 9 and 10 offer a quantitative comparison among various results, where  $\Delta t_s$ (ms) denotes the response time and  $\Delta U_s(\%)$  signifies the voltage overshoot during load shedding tests. These results were achieved through improved tuning of the fuzzy controller. It's worth noting that the response time is gauged at 0.5% of the set-point value. Across different tests, it's evident that the FABE excitation system yields the most favorable outcomes, significantly enhancing the terminal voltage performance of the synchronous generator (SG). Notably, there's a remarkable reduction in both response time and voltage overshoot during load shedding. For instance, during the load shedding 100<sub>0.8</sub> test, the voltage overshoot is approximately 2.09 % when utilizing FABE, whereas it rises to 12% with CBE. This exemplifies a substantial reduction in the response time as well. This underscores the overall superiority of the FABE excitation system in improving system performance across different operational scenarios. Noting that during load impact, the H∞ controller increases the excitation current to regulate the voltage at its rated value (1 p.u.). The CBE and FABE systems yield approximately the same results for stability, voltage drop, and response time.

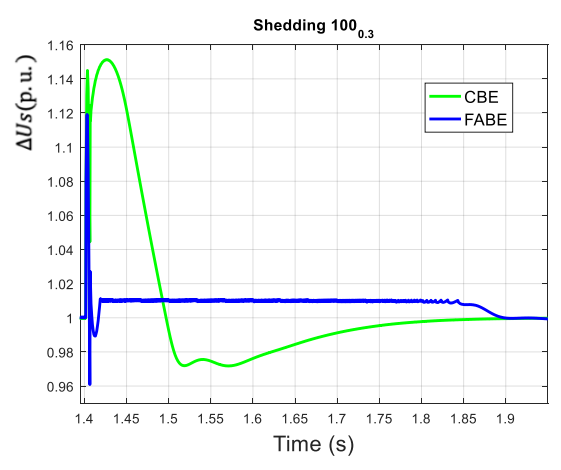


Fig. 5 – R.m.s voltage (p.u.) during the shedding of a load that consumes 100% of the generator's apparent power with a PF=0.3.

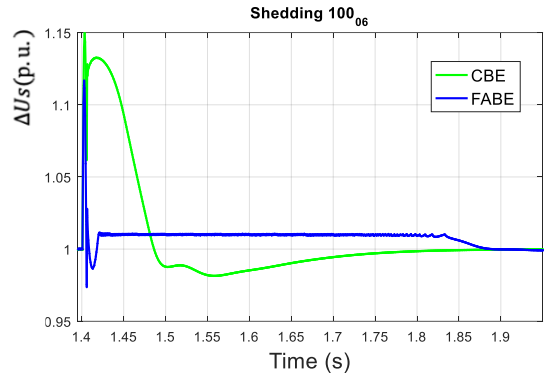


Fig. 6 – R.m.s voltage (p.u.) during the shedding of a load that consumes 100% of the generator's apparent power with a PF = 0.6.

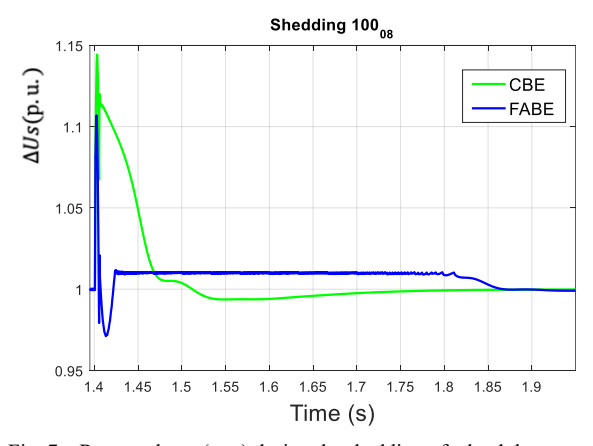


Fig. 7 – R.m.s voltage (p.u.) during the shedding of a load that consumes 100% of the generator's apparent power with a PF = 0.8.

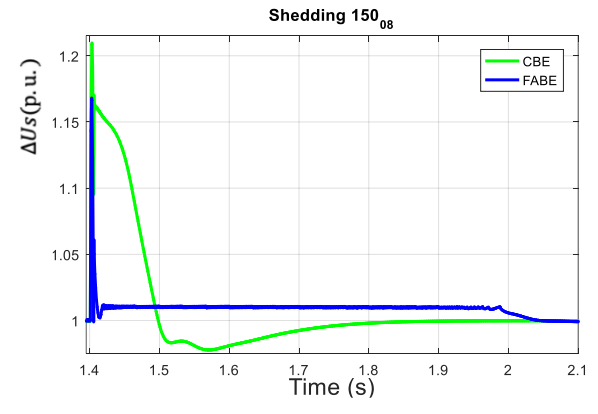


Fig. 8 – R.m.s voltage (p.u.) during the shedding of a load that consumes 150% of the generator's apparent power with a PF=0.8.



Fig. 9 – Results comparison for load shedding tests (voltage overshoot %).

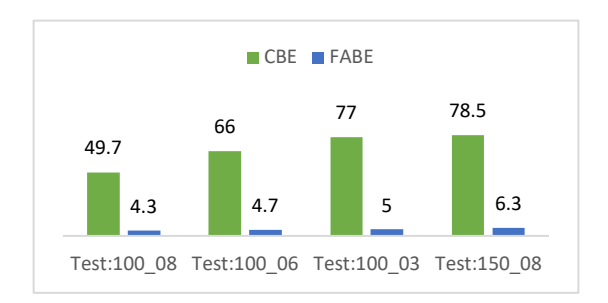


Fig. 10 – Results comparison for load shedding tests (response time in ms).

#### 5. CONCLUSIONS

To enhance the dynamic de-excitation performance and stability of brushless synchronous machines, this research introduces a novel approach. It combines fuzzy logic control with H∞ control to create a new Fuzzy Advanced Brushless Excitation (FABE) control system. In this system, the FLC governs the operation of the rotating IGBT, controlling its opening and closing actions. Additionally, an H∞ control strategy is implemented to specifically address the switching operation of the rotating IGBT. This integrated approach ensures the system's stability within a closed-loop framework, even when the proposed de-excitation system is activated. effectiveness of this advanced control approach was evaluated under several scenarios, demonstrating a significant enhancement in voltage control. Compared with responses obtained using conventional brushless excitation methods, it showed significant improvements in voltage overshoot, response time, and stability.

#### **AUTHOR CONTRIBUTIONS**

Seif E. Chouaba: conceptualization, methodology, formal analysis, visualization, writing – original draft, writing – review & editing. Abdallah Barakat: visualization, writing – original draft, writing – review & editing.

#### **APPENDIX**

Characteristics of the SG							
Poles	$R_s$	$R_f$	$L_f$	$L_d$	$M_{sf}$	$L_q$	
4	0.71	2.06	695	63.6	200.5	38.6	
$L_D$	$L_Q$	$M_{fD}$	$M_{sD}$	$M_{sQ}$	$R_D$	$R_Q$	
0.0685	0.0236	6.7	2	0.9	8.6e-4	9.9e-4	
Characteristics of the EM							
Poles	$R_{se}$	$R_e$	$L_e$	$L_{de}$	$M_{se}$	$L_{qe}$	
8	0.26	24.5	1750	5.8	89	3.1	

#### Received on 10 March 2025

#### REFERENCES

- C.H.T. Lee, K.T. Chau, C. Liu, and C.C. Chan, Overview of magnetless brushless machines, IET Electric Power Appl., 12, pp. 1117–1125 (2018).
- C.A. Platero, M. Redondo, F. Blázquez, and P. Frías, High-speed deexcitation system for brushless synchronous machines, IET Elect. Power Appl., 6, pp. 156–161 (2012).
- E. Rebollo, C.A. Platero, D. Talavera, and R. Granizo, Use of discharge resistor to improve transient de-excitation in brushless synchronous machines, Energies, 12, 13, pp. 2528 (2019).
- E. Rebollo and C.A. Platero, Wireless supervision of a rotating highspeed de-excitation system for brushless SM, In International Conference on Electrical Machines (ICEM), Chalmers in Sweden (2020).
- S.E. Chouaba and A. Barakat, Advanced brushless excitation system with dynamic de-excitation capability, International Review of Electrical Engineering, 14, 2, pp. 1636 (2019).
- S.E. Chouaba and A. Barakat, Controlled brushless de-excitation structure for synchronous generators, Eng. Technol. Appl. Sci. Res., 9, 3, pp. 4218–4224 (2019).
- G.M. Ngaleu, A novel brushless de-excitation system for synchronous generators using a buck chopper with a freewheeling discharge resistor, IET Electr. Power Appl., 17, 3, pp. 314–329 (2023).
- J.K. Nøland, E.F. Alves, A. Pardini, and U. Lundin, Unified reduced model for a dual-control scheme of the high-speed response brushless excitation system of synchronous generators, IEEE Trans. on Industrial Electronics, 67, 6, pp. 4474

  –4484 (2020).
- O.K. Krinah, R. Lalaloul, Z. Ahmida, and S. Oudina, Performance investigation of a wind power system based on double-feed induction generator: fuzzy versus proportional integral controllers, Rev. Roum. Sci. Techn. – Électrotechn. Et Énerg., 67, 4 (2022).
- A. Derbane, B. Tabbache, and A. Ahrichea, Fuzzy logic approach based direct torque control and five-leg voltage source inverter for electric vehicle powertrain, Rev. Roum. Sci. Techn. – Électrotechn. Et Énerg., 66, 1, pp. 15–20 (2021).
- 11. A. Akka, H. Lallouani, O. Moussa, and A. Bouzidi, *Interval type-2 fuzzy logic control for brushless doubly fed induction generator based on wind energy conversion systems*, Rev. Roum. Sci. Techn. Électrotechn. Et Énerg., **70**, *3*, pp. 307–311 (2025).
- C. Mama, A. Chaouch, and B. Benaissa, Comparison of the various controls of the switched reluctance motor 12/8, Rev. Roum. Sci. Techn. – Électrotechn. Et Énerg., 68, 1, pp. 52–57 (2023).
- Kentli, Studies on fuzzy logic control of electrical machines in Turkish Universities: an overview, Mathematical and Computational Applications, 16, 1, pp. 236–247 (2011).
- 14. Hazzab, A. Laoufi, I.K. Bousserhane, and M. Rahli, *Real-time implementation of fuzzy gain scheduling of PI controller for induction machine control*, International Journal of Applied Engineering Research, 1, 1, pp. 51–60 (2006).
- Khelloufi, B. Sari, and S.E. Chouaba, Structured H∞ control-based robust power system stabilizer for stability of multi-machine system, Rev. Roum. Sci. Techn. – Électrotechn. Et Énerg., 69, 1, pp. 91–96 (2024).
- 16. Barakat, S. Tnani, G. Champenois, and E. Mouni, *Monovariable and multivariable voltage regulator design for a synchronous generator modeled with fixed and variable loads*, IEEE Trans. Energy Convers., **26**, *3*, pp. 811–821 (2011).
- R.W. Beaven, M.T. Wright, and D.R. Seaward, Weighting function selection in the H∞ design process, Control Eng. Practice, 4, 5, pp. 625–633 (1996).
- D.W. Gu, P.H. Petkov, and M.M. Konstantinov, Robust control design with MATLAB, Springer, New York (2005).